Materials Transactions, Vol. 61, No. 4 (2020) pp. 766 to 775

Effects of Size of the Largest Crack and Size Difference among Cracks on Critical Current of Superconducting Tape with Multiple Cracks in Superconducting Layer

Shojiro Ochiai[1] and Hiroshi Okuda[2]

[1]*Elements Strategy Initiative for Structural Materials, Kyoto University, Kyoto 606-8501, Japan*
[2]*Department of Materials Science and Engineering, Kyoto University, Kyoto 606-8501, Japan*

The effects of the size of the largest crack and size difference among cracks on critical current of superconducting tape with multiple cracks of different sizes in the superconducting layer were investigated by a model analysis and a Monte Carlo simulation, using the specimens consisting of a series circuit of local sections where each section has one crack of different size from each other. It was revealed that, with increasing distribution-width of crack size, the increase in the size of the largest crack acts to reduce the critical current and the increase in the crack size-difference among the sections acts to raise the critical current, and these conflicting two effects are summed up and determine the critical current value. To describe this feature quantitatively, we expressed the statistics of the size of the largest crack in specimens with the Gumbel's extreme value distribution function. Also we monitored the effect of the difference in crack size among the sections on specimen's critical current, using the number of the sections equivalent to the largest crack-section at the critical voltage for determination of specimen's critical current. In this monitoring, small number of the sections equivalent to the largest crack-section corresponds to large difference in crack size among the sections. With the present approach, the effect of the increase in size of the largest crack, which acts to reduce critical current, and the effect of the increase in difference in crack size among the sections, which acts to raise critical current, with increase in distribution-width of crack size, could be estimated separately. [doi:10.2320/matertrans.MT-MBW2019001]

(Received October 21, 2019; Accepted December 10, 2019; Published January 20, 2020)

Keywords: *superconducting tape, critical current, largest crack, size difference among cracks, model analysis, simulation*

1. Introduction

During fabrication and operation, superconducting tapes are subjected to thermal, mechanical, and electromagnetic stresses/strains. At high stresses/strains, the superconducting phase is cracked, which reduces critical current I_c and n-value in both coated[1–12] and filamentary[13–21] tapes. Cracking of the superconducting layer/filament occurs heterogeneously, due to which the I_c- and n-values differ from specimen to specimen[6–12] and vary along the specimen length.[7–12,14,15] The same situation takes place under the existence of the heterogeneously distributed I_c-reducing defects, introduced during the tape-fabrication process.[22,23] It is required to have full knowledge of the relation of heterogeneously distributed defects/cracks to superconducting property for safety design.

We have been developing a Monte Carlo simulation method[7–12] combined with the current shunting model at cracks[13] to detect the effects of crack size distribution on I_c- and n-values. We have shown that, among the voltage V–current I curves of the local sections that constitute the specimen, the V–I curve of the section with the largest crack contributes most to the synthesis of the V–I curve of the specimen.[9–12] Accordingly, the size of the largest crack is a primary factor in determination of I_c-value of specimen. However, not only the size of the largest crack but also the difference in crack size among the sections affects the I_c-value of specimen,[9–12] since the latter changes the interspacing among the V–I curves of the local sections and hence the V–I curve of the specimen.[9,12]

In the present work, we took up the stress-induced cracks as the representative of the defects, and attempted to describe the I_c values from the viewpoint of the roles of the size of the largest crack and the size difference among the cracks in determination of the specimen's I_c values. As the tools, we used the Monte Carlo simulation method mentioned above, Gumbel's extreme value distribution[24] for calculation of the size-distribution of the largest crack among the specimens and a new method that monitors the effect of the size difference among the cracks on the specimen's I_c values. Details of the procedure of the simulation and analysis, and the results, are reported in this paper.

2. Procedure of Simulation and Model Analysis

2.1 Model specimen consisting of local sections

RE(Y, Sm, Dy, Gd, ...)$Ba_2Cu_3O_{7-\delta}$ layer-coated superconducting tape (hereafter noted as REBCO tape) was used for the model specimen whose configuration is shown in Fig. 1(a) and (b). The specimens were 4.5, 15 and 30 cm long, consisting of 3, 10 and 20 local sections with a length $L_0 = 1.5$ cm. Each section had one crack with a different size from each other. Current path in a cracked section is shown schematically in Fig. 2, in which one section in a REBCO tape specimen is representatively drawn. In the transverse cross-section in which a crack exists, the cracked part and the ligament part constitute a parallel electric circuit.

2.2 Procedure of the Monte Carlo simulation to obtain the critical current values of the sections and specimens

Details of the simulation procedure have been reported in our preceding works.[7–12] Here, we show an outline. The following technical terms were used.

f and $1-f$: ratios of cross-sectional area of the cracked part and ligament part to the total cross-sectional area of the REBCO layer, respectively.
I_{RE}: current transported by the REBCO layer in the ligament part.
I_s: crack-induced shunting current at the cracked part.
R_t: electric resistance of the shunting circuit.
V_{RE}: voltage developed at the ligament part that transports the current I_{RE}.

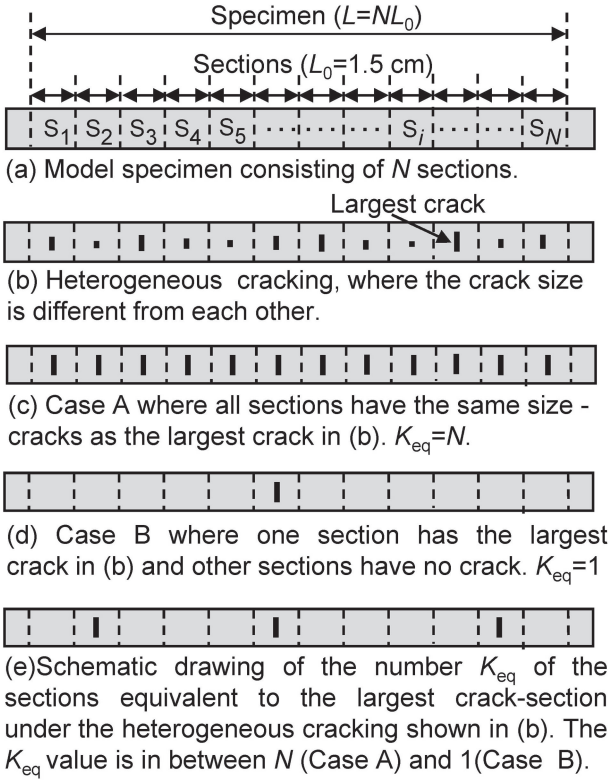

Fig. 1 Modeling for analysis. (a) The model specimen consisting of N local sections with a length $L_0 = 1.5$ cm, having a crack in each section. (b) Configuration of multiple cracks of different sizes in specimen. (c) An extreme Case A (N sections have the same size-crack). (d) Another extreme Case B (one section has a crack and other sections have no crack). (e) Schematic drawing of the number of sections equivalent to the largest crack-section K_{eq} ($1 \le K_{eq} \le N$), which is used to monitor the effect of the difference in crack size among the sections shown in (b) on critical current of the specimen. The case of $K_{eq} = 3$ is drawn as an example.

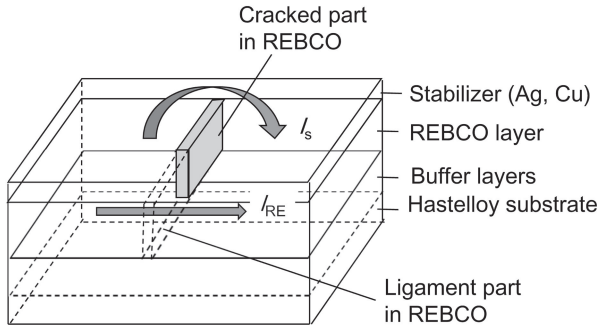

Fig. 2 Schematic representation of the current path in a section with a crack.[7)]

V_s ($= I_s R_t$): voltage developed at the cracked part due to the shunting current I_s.
I_{c0} and n_0: critical current and n-value of the sections in the non-cracked state, respectively.
E_c ($= 1\,\mu V/cm$): critical electric field at which the I_c-value is determined.
s ($\ll L_0$): current transfer length.
L_p: ligament parameter of section given by $L_p = (1 - f)(L_0/s)^{1/n_0}$, which was derived by the authors[2,4,7–12)] through a modification of the formulations of Fang *et al.*[13)]

The cracked- and ligament-parts constitute a parallel electric circuit in the cracked section.[13)] Accordingly, the voltage V_s developed at the cracked part is equal to the voltage V_{RE} developed at the ligament part ($V_s = V_{RE}$). In this work, we use V_{RE} as a representative of V_{RE} and V_s. The transport current I is the sum of the REBCO-transported current I_{RE} in the ligament part and the shunting current I_s in the cracked part ($I = I_{RE} + I_s$).

The V–I curve of the cracked section is expressed as,[2,3,9–12)]

$$V = E_c L_0 \left(\frac{I}{I_{c0}}\right)^{n_0} + V_{RE} \tag{1}$$

$$I = I_{RE} + I_s = I_{c0} L_p \left[\frac{V_{RE}}{E_c L_0}\right]^{1/n_0} + \frac{V_{RE}}{R_t} \tag{2}$$

The ligament parameter L_p ($= (1 - f)(L_0/s)^{1/n_0}$) in eq. (2) was used to monitor the ligament area fraction $1 - f$. It was used also as a monitor of the crack area fraction f, since f has one to one correspondence with $1 - f$, showing the following features. (i) Small/large ligament area fraction $1 - f$ corresponds to large/small crack area fraction f; namely, the smaller the ligament parameter, the larger is the crack. (ii) The standard deviation of the ligament area fraction $1 - f$ is the same as that of the crack area fraction f. Hence, the standard deviation of L_p, ΔL_p, was used as a monitor of the distribution-width of ligament size as well as the distribution-width of crack size; the larger the ΔL_p-value, the wider is the crack size distribution and also the wider is the ligament size distribution.

The distribution of L_p was formulated using the normal distribution function, as in our former works.[9–12)] The cumulative probability $F(L_p)$ and density probability $f(L_p)$ for the average of L_p, $L_{p,ave}$, are expressed as

$$F(L_p) = \frac{1}{2}\left\{1 + \mathrm{erf}\left(\frac{L_p - L_{p,ave}}{\sqrt{2}\Delta L_p}\right)\right\} \tag{3}$$

$$f(L_p) = \frac{1}{\sqrt{2\pi}\Delta L_p} \exp\left\{-\frac{(L_p - L_{p,ave})^2}{2(\Delta L_p)^2}\right\} \tag{4}$$

The $L_{p,ave}$ was taken to be 0.67 which refers to the situation where the average critical current $I_{c,ave}$ of the sections is reduced to $\approx 2/3$ from the non-cracked state.[7)] To obtain the distribution of I_c values under wide variety of the distribution-width of crack size, five cases of $\Delta L_p = 0.01$, 0.025, 0.05, 0.10 and 0.15 were taken up. The L_p value was given for each cracked section with a Monte Carlo method.[7–12)]

The V–I curve of each cracked section was calculated, by substituting the L_p-value obtained by the Monte Carlo method, and the values of $I_{c0} = 200$ A, $n_0 = 40$ and $R_t = 2\,\mu\Omega$, taken from our former experimental work on REBCO tape,[5,9–12)] into eqs. (1) and (2).

As the specimen consists of a series electric circuit of N sections ($N = 3$, 10 and 20 for $L = 4.5$, 15 and 30 cm, respectively) (Fig. 1(a)), the current in the specimen is the same as that in all sections, and the specimen's voltage is the sum of the voltages of all sections,

$$I_{specimen} = I_{section(i)} \quad (i = 1 \text{ to } N) \tag{5}$$

$$V_{\text{specimen}} = \sum_{i=1}^{N} V_{\text{section}(i)} \quad (6)$$

Using the V–I curves of the sections, the V–I curve of the specimen was obtained with eqs. (5) and (6).

From the V–I curves of the sections and specimens, the I_c-values of the sections and specimens were obtained with the electric field criterion of $E_c = 1\,\mu\text{V/cm}$, corresponding to the critical voltages $V_c = E_c L_0$ for sections and $V_c = E_c L = E_c N L_0$ for specimens.

2.3 Model to obtain the upper and lower bounds of critical current of specimens[9–12)]

The present model specimen consists of a series of N sections and contains N cracks of different sizes (Fig. 1(b)). The superconductivity is lost first in the section with the largest crack. Therefore, the voltage developed at the largest crack-section is the highest among all sections, and it contributes most to the specimen's voltage. We can obtain the upper and lower bounds of I_c of specimen using the V–I curve of the largest crack-section among all sections, as follows.[9–12)] Hereafter the ligament parameter of the largest crack-section (= smallest ligament-section) among all sections is expressed as $L_{\text{p,smallest}}$.

Case A (Fig. 1(c)) corresponds to the extreme case where the crack size is the same as the largest crack in all sections. Thus, the V–I curves of all sections are the same. Accordingly, the specimen's voltage, given by the sum of the voltage of all sections, corresponds to the upper bound of the specimen's voltage, V_{upper}, under the given size of the largest crack. As the V_{upper} reaches the critical voltage V_c at lowest I, the I_c value in Case A corresponds to the lower bound, $I_{\text{c,lower}}$.

Case B (Fig. 1(d)) corresponds to the extreme case where the specimen is an assembly of one severely cracked section and non-cracked sections. This case gives the lower bound V_{lower} for the specimen's voltage under the given size of the largest crack. As V_{lower} reaches V_c at highest I, the I_c value in Case B corresponds to the upper bound $I_{\text{c,upper}}$.

Case A gives the V_{upper}–I curve and $I_{\text{c,lower}}$, and Case B gives the V_{lower}–I curve and $I_{\text{c,upper}}$ for specimen under the given size of the largest crack (= smallest ligament). The V_{upper}–I and V_{lower}–I curves of specimens were calculated with eqs. (1), (2), (5) and (6) by setting $L_p = L_{\text{p,smallest}}$ that refers to the smallest ligament (= largest crack)-section. From the calculated curves, the $I_{\text{c,upper}}$ and $I_{\text{c,lower}}$ values were obtained with the criterion of $E_c = 1\,\mu\text{V/cm}$.

2.4 Monitoring of the contribution of the difference in crack size among sections to the critical current of specimen

In Case A, number of N sections have the largest crack (Fig. 1(c)), and, in Case B, one section has the largest crack (Fig. 1(d)). In practical situation as shown in Fig. 1(b), not only the largest crack-section but also the other sections contribute to the voltage of the specimen. In this study, for the quantitative estimation of the effect of the positional relation of the V–I curves of the sections, induced by the difference in crack size among the sections, on the critical current of specimens, the sum of the voltages of sections (= the voltage of the specimen) was replaced by the sum of the voltages of a number of K_{eq} sections equivalent to the largest crack-section and the voltages of N–K_{eq} sections without cracks. As an example of this replacement, the case of $K_{\text{eq}} = 3$ is shown schematically in Fig. 1(e) where the voltage of the specimen at $V = V_c$, which is the sum of the voltages of the sections containing the cracks of different sizes in Fig. 1(b), is expressed as the sum of the voltages of K_{eq} (= 3) sections equivalent to the largest crack-section and voltages of N–K_{eq} non-cracked sections at $V = V_c$. In this approach, the V–I curves of the largest crack-section could be expressed by eqs. (1) and (2) as before, and the V–I curve of the specimen can be expressed by.

$$V = E_c L \left(\frac{I}{I_{c0}}\right)^{n_0} + K_{\text{eq}} V_{\text{RE}} \quad (7)$$

The K_{eq} is large when the V–I curves of the sections are dense in narrow current range (= when the difference in crack size among the sections is small) and it is small when the V–I curves of sections are apart from each other (= when the difference in crack size among the sections is large).

Figure 3 shows the difference in I_c value due to the difference in K_{eq} value under the condition of the smallest ligament parameter $L_{\text{p,smallest}} = 0.5$ and specimen length $L = 15\,\text{cm}$, as an example. The V–I curves of the specimen for $K_{\text{eq}} = 1$ to 10 are shown in Fig. 3(a), in which $K_{\text{eq}} = 10$ and 1 corresponds to Cases A and B, respectively. The K_{eq} value exists in between 1 and N ($= L/L_0$), as schematically

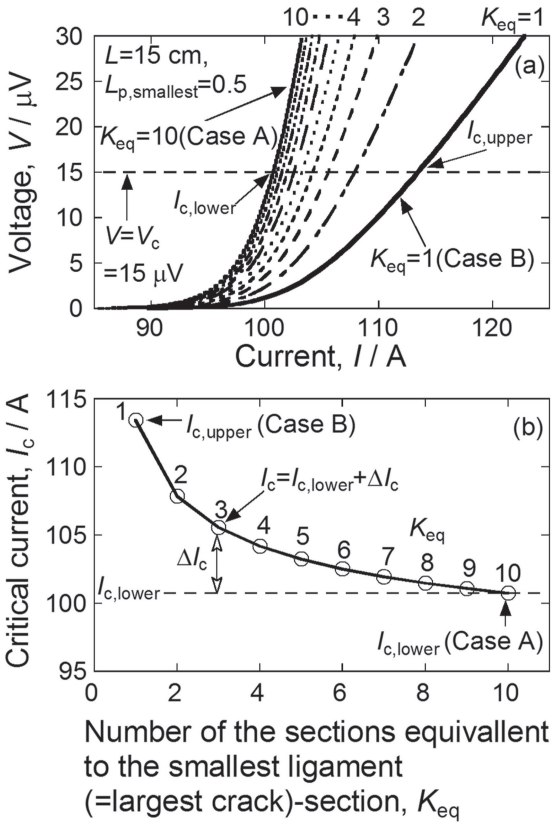

Fig. 3 An example showing the effects of K_{eq} value on critical current. (a) V–I curves of the specimen for $K_{\text{eq}} = 1$ to 10, in which $K_{\text{eq}} = 10$ and 1 corresponds to Cases A and B, respectively and (b) change in critical current of the specimen with varying K_{eq} value, calculated for the smallest ligament parameter $L_{\text{p,smallest}} = 0.5$ and specimen length $L = 15\,\text{cm}$.

shown in Fig. 1(c–e). The I_c value of the 15 cm-specimen is equal to $I_{c,lower}$ when $K_{eq} = N = 10$ (Case A), it increases with decreasing K_{eq} and becomes the upper bound value $I_{c,upper}$ when $K_{eq} = 1$ (Case B), as shown in Fig. 3(b).

The results in Fig. 3(b) show evidently that the I_c value increases with decreasing K_{eq}; namely with increasing difference in crack size among the sections under the given size of the largest crack (= under the given size of the smallest ligament, which is given by $L_{p,smallest} = 0.5$ in this example). In this way, the I_c value is affected not only by the size of the largest crack that is monitored by $L_{p,smallest}$ but also by the difference in crack size among the sections that is monitored by K_{eq}. It is noted that, while the I_c value is dependent both on $L_{p,smallest}$- and K_{eq}-values, the $I_{c,lower}$ value (Case A) is determined solely by the $L_{p,smallest}$ value, as will be shown in detail in subsection 3.1. The difference ΔI_c between the I_c and $I_{c,lower}$, $\Delta I_c = I_c - I_{c,lower}$, is attributed to the effect of the difference in crack size among the sections. As an example, the case of $K_{eq} = 3$ is picked up and the ΔI_c and its relation to I_c and $I_{c,lower}$ are drawn in Fig. 3(b). In this way, I_c is given by the sum of the effect of the largest crack size ($I_{c,lower}$) and that of the difference in crack size among the sections (ΔI_c). This result will be used in subsections 3.1 and 3.2 for separate estimation of the effects of the size of the largest crack and the difference in crack size among sections on I_c value.

Figure 4 shows the examples showing the effect of difference in crack size among the sections in 15 cm-specimen constituted of 10 sections (a, a′) on the positional relation of the *V–I* curves among the sections and between the specimen and the sections, (b, b′) on the positional relation among the *V–I*, V_{upper}–*I* and V_{lower}–*I* curves of specimen, and (c, c′) on the positional relation of the *V–I* curve of the specimen obtained by simulation and the *V–I* curves of the specimen calculated with eqs. (1), (2) and (7) for $K_{eq} = 1$ to 10, where $K_{eq} = 1$ and 10 refer to Case B and Case A, respectively. The results of the examples Ex. 1 in Fig. 4(a–c) and Ex. 2 in Fig. 4(a′–c′), taken up from the simulation results, correspond to the cases where the difference in ligament parameter (L_p) value (= difference in crack size) among the sections is small and large, respectively. In these examples, the average of the ligament parameter, $L_{p,ave}$, (namely average of crack size) was common ($L_{p,ave} = 0.67$) and the distribution-width of crack size was different.

When the crack sizes of the sections are close to each other as in Ex. 1, the *V–I* curves of all sections exist near to the *V–I* curve of the largest crack-section. Therefore, the voltages of many sections contribute to the rise of the voltage of the specimen. On the other hand, when the crack sizes of the sections are different as in Ex. 2, the interspacing among the *V–I* curves of the sections is large. Therefore, the voltage only of the largest crack-section or a few sections with the relatively large cracks contributes to synthesize the *V–I* curve of the specimen. The critical currents of the extreme Cases A and B are obtained from the V_{upper}–*I* and V_{lower}–*I* curves, respectively. In actual specimens, the situation is in between Case A and Case B, and accordingly the *V–I* curves exist in between the V_{upper}–*I* and V_{lower}–*I* curves, and the critical current values exist in between Case A and Case B (Fig. 3(a, b)).

The I_c value of specimen is given as the current at $V = V_c = E_c L$. The relation of V_c to I_c, K_{eq} and V_{RE} and the relation of I_c to $L_{p,smallest}$ and V_{RE} in the smallest ligament-section are expressed by eqs. (8) and (9) from eqs. (7) and (2), respectively:

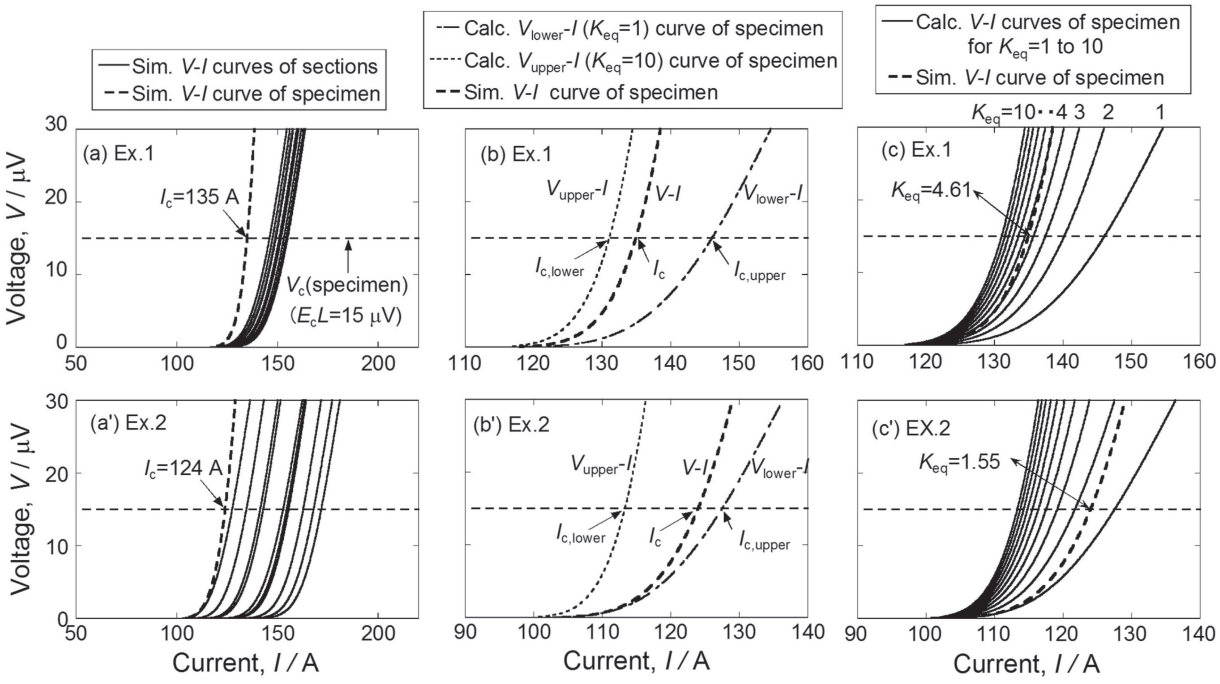

Fig. 4 Effect of difference in crack size among the sections on the *V–I* curve and critical current of specimen. Ex. 1 and Ex. 2 are examples taken from the simulation results, where the difference in crack size among the sections is small in Ex. 1 but large in Ex. 2, while the average crack size is common. (a, a′) show the positional relation of the *V–I* curves among the sections and between the specimen and the sections, (b, b′) comparison of the simulated *V–I* curves of specimens with the calculated V_{upper}–*I* and V_{lower}–*I* curves, and (c, c′) comparison of the simulated *V–I* curves of specimens with the calculated *V–I* curves for $K_{eq} = 1$ to 10.

$$V_c = E_c L = E_c L\left(\frac{I_c}{I_{c0}}\right)^{n_0} + K_{eq} V_{RE} \quad (8)$$

$$I_c = I_{RE} + I_s = I_{c0} L_{p,\,smallest}\left[\frac{V_{RE}}{E_c L_0}\right]^{1/n_0} + \frac{V_{RE}}{R_t} \quad (9)$$

K_{eq} value at $V = V_c$ for each specimen can be obtained as the value that satisfies eqs. (8) and (9). Substituting the values of I_c and $L_{p,smallest}$ obtained by simulation whose details will be presented later in the subsection 3.1 and the known values of I_{c0}, n_0, R_t, E_c and L into eqs. (8) and (9), we obtained the K_{eq} value for each specimen. The obtained K_{eq} values for Ex. 1 and Ex. 2 were 4.61 and 1.55 as shown in Figs. 4(c) and 4(c′), respectively. It is noted that K_{eq} value is not necessarily an integer. As long as the K_{eq} value satisfies eqs. (8) and (9), it is hold mathematically even if the values below the decimal point are included.

When the distribution-width of the crack size is small as in Ex. 1, K_{eq} value is high (4.61). With increasing distribution-width of crack size, K_{eq} value decreases (1.55 in Ex. 2) and asymptotically approaches unity at large difference in crack size among the sections (Fig. 3(b)). With the present approach, K_{eq} values for wide range of ΔL_p and L can be obtained.

3. Results and Discussion

3.1 Role of the size of the largest crack in determination of critical current of specimen

Figure 5 shows the changes of (a–c) the smallest ligament parameter $L_{p,smallest}$ values and (a′–c′) critical current I_c values of specimens with increase in standard deviation of the ligament parameter ΔL_p, obtained by simulation for specimen length L = (a, a′) 4.5 cm, (b, b′) 15 cm and (c, c′) 30 cm. The circle (○) indicates the value of $L_{p,smallest}$ and I_c of each specimen, and the square (□) indicates the average value ($L_{p,smallest,ave}$ and $I_{c,ave}$). Evidently, the $L_{p,smallest,ave}$ and $I_{c,ave}$ of specimens decreased with increasing ΔL_p. Also the extent of their decrease with increasing ΔL_p was enhanced in longer specimen. These results suggest that, on average, the size of the smallest ligament in specimen decreases (= size of the largest crack in specimen increases) with increasing ΔL_p and L, which acts to reduce I_c.

Figure 6 shows the plot of (a–c) I_c value of each specimen against the $L_{p,smallest}$ value, and plot of (a′–c′) $I_{c,ave}$ value of specimens against the $L_{p,smallest,ave}$ value, where the I_c and $L_{p,smallest}$ values were averaged for each set of L- and ΔL_p-values. The lower bound $I_{c,lower}$ and upper bound $I_{c,\,upper}$ of critical current were obtained as a function of $L_{p,smallest}$ through the calculation of the V–I curves, by setting $L_p = L_{p,smallest}$ in eq. (2) and $K_{eq} = N$ (Case A) and 1 (Case B) in eq. (7).

The results in Fig. 6 show that, when the specimen is short (4.5 cm), the difference between $I_{c,upper}$ and $I_{c,lower}$ is small. This feature suggests that the smallest ligament (= largest crack)-section plays a significant role in determination of I_c-value especially in short specimens, as has been shown in our preceding work.[12] When the $I_{c,upper}$–$I_{c,lower}$ is small as in Fig. 6(a, a′), the I_c is approximately expressed as[12]

$$I_c \cong I_{c,\,lower} \quad (10)$$

When the specimen is long (30 cm), the largest crack-section still plays a major role in determination of I_c value. However, as shown in Fig. 6(c, c′), the difference $I_{c,upper}$–$I_{c,lower}$ becomes larger for larger L, and accordingly not only the largest crack but also the difference in crack size among the sections play important roles in determination of I_c value.

When the $L_{p,smallest}$ value is known, $I_{c,lower}$ can be calculated under the condition of $K_{eq} = N$. As shown in our preceding work,[12] the $L_{p,smallest}$-value and its distribution can be obtained by using the Gumbel's extreme value distribution function.[24] The average of $L_{p,smallest}$ values of the specimens, $L_{p,smallest,ave}$, for each set of ΔL_p- and L-values is obtained by[24]

$$L_{p,smallest,ave} = \lambda - \alpha\gamma \quad (11)$$

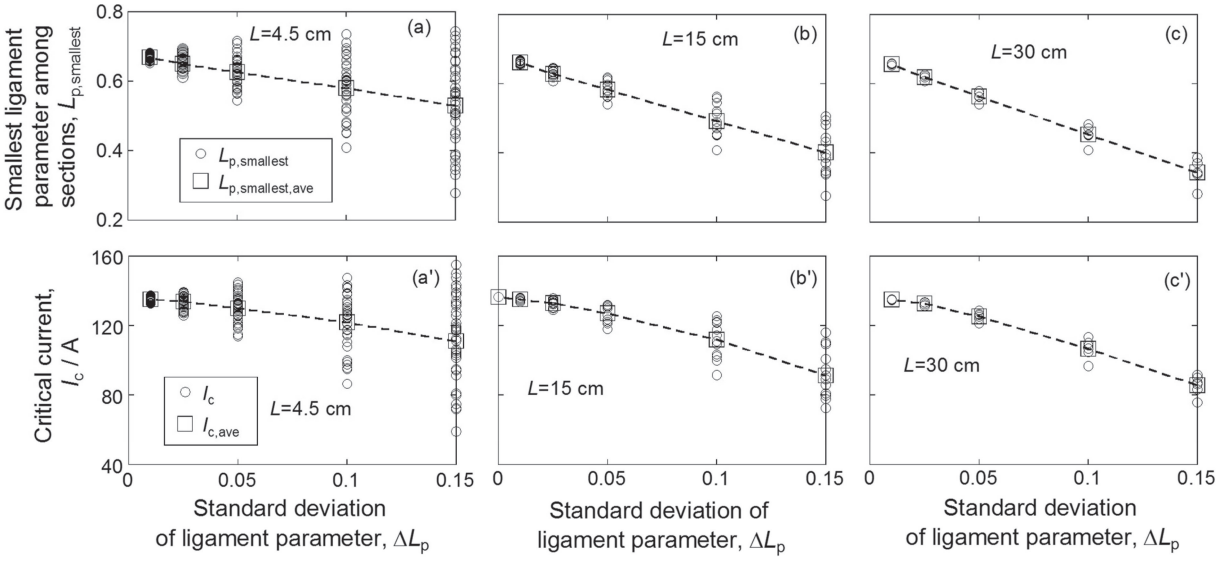

Fig. 5 Changes of (a–c) the smallest ligament parameter $L_{p,smallest}$ and (a′–c′) critical current I_c of the specimens with increasing standard deviation of the ligament parameter ΔL_p, obtained by simulation for specimen length L = 4.5, 15 and 30 cm. The circle symbol indicates the value of each specimen and the square symbol indicates the average value.

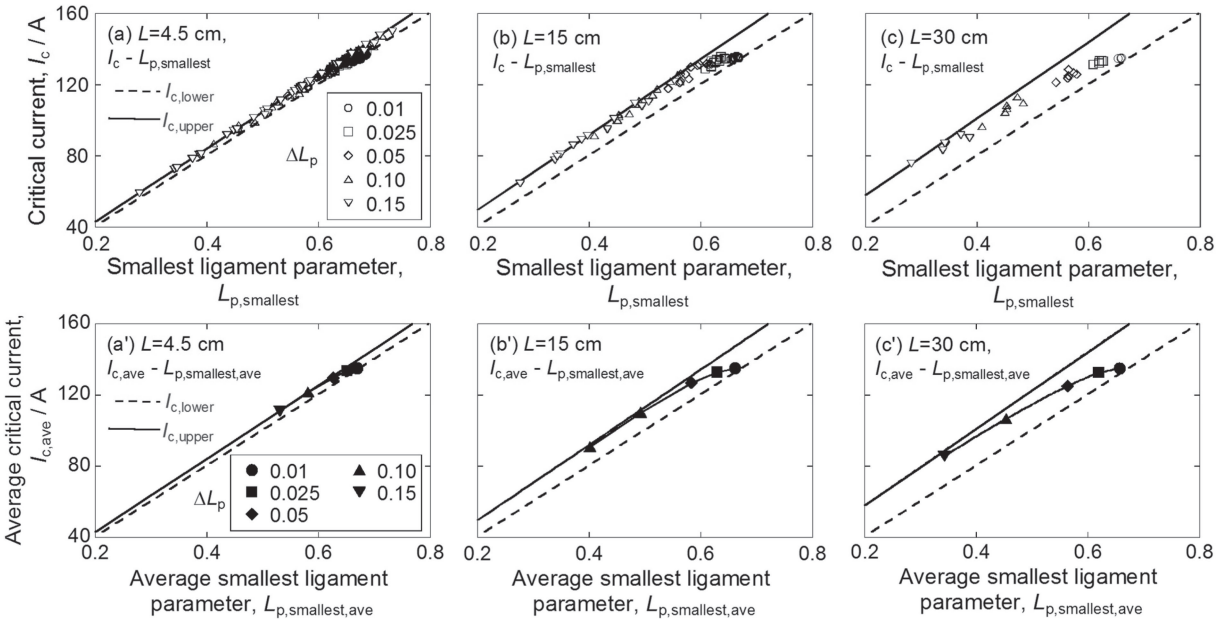

Fig. 6 Plot of (a–c) critical current I_c against the smallest ligament parameter $L_{p,smallest}$, and (a′–c′) average critical current $I_{c,ave}$ against the average smallest ligament parameter $L_{p,smallest,ave}$. (a, a′), (b, b′) and (c, c′) refer to the simulation results for $L = 4.5$, 15 and 30 cm, respectively. For comparison, the calculated relations of $I_{c,upper}$ to $L_{p,smallest}$ and $I_{c,lower}$ to $L_{p,smallest}$ are presented with the solid and broken lines, respectively.

where γ is the Euler-Mascheroni constant ($= 0.5772$), λ is the positional parameter and α is the scale parameter in the extreme value distribution function.[24] By using the cumulative distribution function of L_p, $F(L_p)$ (eq. (3)), and the probability density function of L_p, $f(L_p)$ (eq. (4)), λ and α can be obtained as the values that satisfy the following formulations.[24]

$$F(\lambda) = 1/N \tag{12}$$

$$\alpha = 1/\{Nf(\lambda)\} \tag{13}$$

We calculated $L_{p,smallest,ave}$ value using eqs. (3), (4), (11), (12) and (13) under the condition of $\Delta L_p = 0.01$, 0.025, 0.05, 0.10 and 0.15, and $L = 4.5$, 15 cm and 30 cm. Figure 7(a) show the plots of $L_{p,smallest,ave}$ value obtained by simulation (open symbols) and by calculation (closed symbols), against ΔL_p value. The values of $L_{p,smallest,ave}$ obtained by simulation were well described by calculation. In this way, the $I_{c,lower,ave}$ value can be obtained by calculation of the V–I curve of specimen by substituting the calculated $L_{p,smallest,ave}$-value, L-value and $K_{eq} = N = L/L_0$ into eqs. (2) and (7) and application of $E_c = 1\,\mu V/cm$ criterion. The calculated and simulated $I_{c,lower,ave}$ values plotted against ΔL_p are shown in Fig. 7(b). The simulation results (open symbols) are well described by calculation (closed symbols).

It is important that the largest crack, monitored by $L_{p,smallest}$, plays a role to give the $I_{c,lower}$, as shown in Fig. 7(c), where the $I_{c,lower,ave}$ values in Fig. 7(b) are plotted against the corresponding $L_{p,smallest,ave}$ values in Fig. 7(a). The $I_{c,lower,ave}$ has one to one relation to the $L_{p,smallest,ave}$ regardless the values of the specimen length L and distribution-width of crack size ΔL_p. The $I_{c,lower,ave}$ arises in Case A where the crack size is the same in all sections in specimen, and hence the $I_{c,lower,ave}$ is not dependent on specimen length. This result shows that the $I_{c,lower,ave}$ value is determined solely by the size of the largest crack. The decrease in critical current with increasing ΔL_p and L is caused by the increase in the size of the largest crack. It is also important that, while the critical current is almost the same as the lower bound when ΔL_p and L are small, the difference between I_c and $I_{c,lower}$, $\Delta I_c = I_c - I_{c,lower}$, increases with increasing ΔL_p and L (Fig. 6). As indicated in Figs. 3 and 4, the wider distribution of crack size, which corresponds to smaller K_{eq} value, leads to wider positional spacing among the V–I curves of sections, which acts to raise I_c value under the given size of the largest crack. Namely, I_c is given by the sum of the $I_{c,lower}$ that is determined by the size of the largest crack and ΔI_c that is determined by the difference in crack size among the sections, as has been shown in Fig. 3(b). In the next subsection, the effect of the difference in crack size among the sections on ΔI_c is evaluated by using the K_{eq}-value.

3.2 Role of the difference in crack size among the sections in determination of critical current of specimen

Figure 8 shows the changes in number of sections equivalent to the largest crack-section, K_{eq}, and the difference between the critical current and its lower bound ($\Delta I_c = I_c - I_{c,lower}$) with increase in distribution-width of crack size (ΔL_p). The values of K_{eq} were estimated by the procedure stated in subsection 2.4. The variations of K_{eq} and $K_{eq,ave}$ (average of K_{eq}-values at each set of ΔL_p- and L-values) with increasing ΔL_p for $L = 4.5$, 15 and 30 cm are shown in Fig. 8(a–c). The K_{eq} decreases with increasing ΔL_p. This decrease reflects the shift of interspacing among the V–I curves of the sections, from narrow interspacing that gives a large K_{eq} value, to wide interspacing that gives a small K_{eq} value.

The values of ΔI_c ($= I_c - I_{c,lower}$) were taken from the simulation results for each ΔL_p value in Fig. 6. The increments of ΔI_c value with increasing ΔL_p for $L = 4.5$, 15 and 30 cm are shown in Fig. 8(a′–c′). The results show

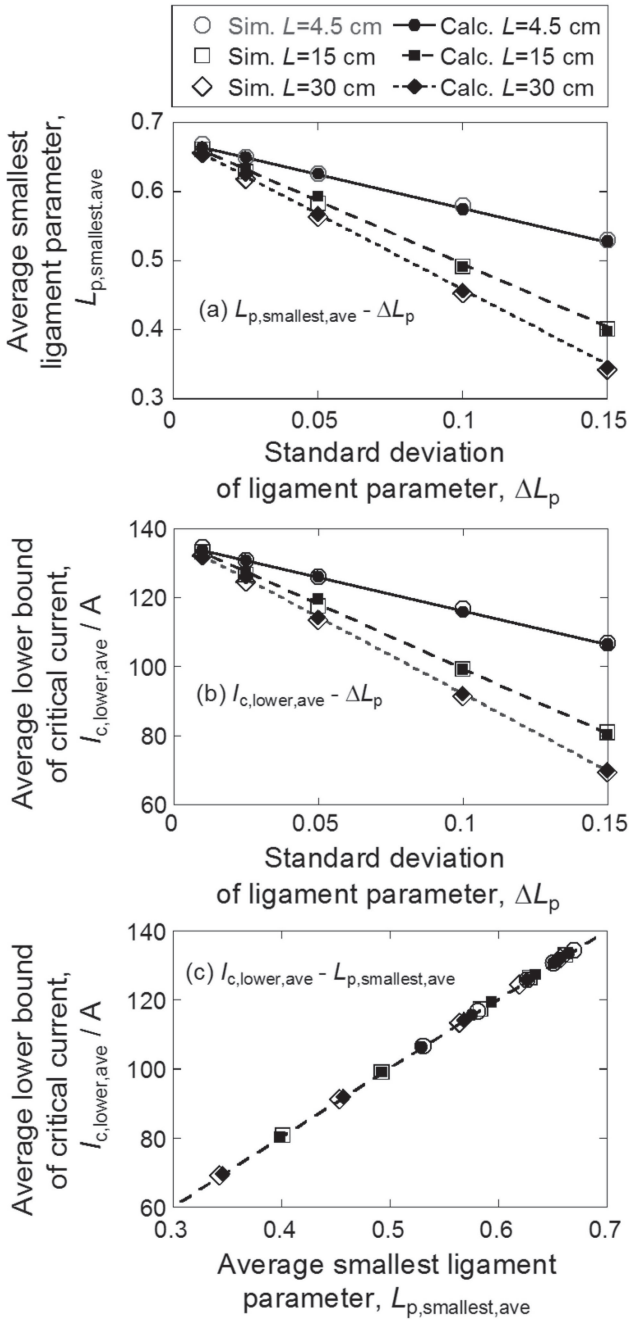

Fig. 7 Plots of (a) average smallest ligament parameter, $L_{p,smallest,ave}$, and (b) average lower bound of critical current $I_{c,lower,ave}$, of the specimens with length $L = 4.5$, 15 and 30 cm, against the standard deviation of ligament parameter ΔL_p. (c) Plots of $I_{c,lower,ave}$ against $L_{p,smallest,ave}$. Open and closed symbols refer to the values obtained by simulation and calculation, respectively.

that the ΔI_c increases with increasing ΔL_p; the larger the difference in crack size among sections, the larger becomes the increment of ΔI_c.

Figure 9 shows the plot of the average values of ΔI_c, $\Delta I_{c,ave}$, at $\Delta L_p = 0.01 \sim 0.15$ against the average of the equivalent number of the largest crack-section, $K_{eq,ave}$, for $L = 4.5$, 15 and 30 cm. The feature that the decrease in K_{eq} contribute to raise ΔI_c for a given $L_{p,smallest}$ value (Figs. 3 and 4) is reproduced well. This result shows that K_{eq} value is useful as a tool to estimate the contribution of the difference in crack size among the sections in determination of ΔI_c.

3.3 Reproduction of the simulation result and analysis of the increment of critical current induced by the difference in crack size among the sections

As has been shown in subsections 3.1 and 3.2, the smallest ligament parameter $L_{p,smallest}$ referring to the largest crack-section and the number of the sections equivalent to the largest crack-section K_{eq} are useful tools to estimate the lower bound of the critical current $I_{c,lower}$ and the contribution of difference in crack size among the sections to critical current ΔI_c, respectively. When the K_{eq}- and $L_{p,smallest}$-values are known by simulation or calculation, the critical current I_c is calculated by $I_c = I_{c,lower} + \Delta I_c$. In this subsection, the simulation results of the changes in $I_{c,ave}$-, $I_{c,lower,ave}$- and $\Delta I_{c,ave}$-values as a function of the distribution-width of ligament size (= distribution-width of crack size) ΔL_p for each specimen length L (4.5, 15 and 30 cm) will be reproduced.

For reproduction of the simulation results, the following calculations were carried out. The $L_{p,smallest,ave}$ values for $\Delta L_p = 0.01 \sim 0.15$ under the specimen length of $L = 4.5$, 15 and 30 cm were calculated using eqs. (3), (4), (11), (12) and (13), as has been shown in Fig. 7. The $I_{c,lower,ave}$ value for each set of ΔL_p- and L-values was obtained by calculation of the V–I curve through substituting the $L_{p,smallest,ave}$ and $K_{eq} = N$ into eqs. (2) and (7) and application of the criterion of $E_c = 1\,\mu V/cm$. In the same way, the $I_{c,ave}$ value was obtained by substituting $L_{p,smallest} = L_{p,smallest,ave}$ and $K_{eq} = K_{eq,ave}$ into eqs. (2) and (7). The $\Delta I_{c,ave}$ was calculated by $\Delta I_{c,ave} = I_{c,ave} - I_{c,lower,ave}$.

Figure 10 shows the changes of the $I_{c,ave}$ values obtained by simulation (○) and calculation (●), the $I_{c,lower,ave}$ values obtained by calculation (◇), and the $\Delta I_{c,ave}$ values obtained by calculation (□) with increasing ΔL_p for $L = 4.5$, 15 cm and 30 cm. As shown in Fig. 10, the simulation results of $I_{c,ave}$ values are described well by the calculation of $I_{c,ave} = I_{c,lower,ave} + \Delta I_{c,ave}$ where the $I_{c,lower,ave}$-value is determined solely by the $L_{p,smallest,ave}$ value and the $\Delta I_{c,ave}$ value is determined by the difference in crack size among the sections under the given value of $L_{p,smallest,ave}$. In this way, the role of the largest crack size and that of the difference in crack size among the sections in determination of critical current are separately estimated by the present approach.

With increase in distribution-width of crack size, the increase in size of the largest crack acts to reduce the critical current, while the increase in the difference in crack size among the sections acts to raise the critical current. The sum of these conflicting effects determines the critical current. The present approach, using the ligament parameter to monitor the crack size and the number of sections equivalent to the largest crack-section to monitor the effect of the difference in crack size among the sections on critical current, can be a useful tool for estimation of critical current of the tape with heterogeneous cracks in the superconducting layer.

3.4 Analysis of the increment of critical current induced by the difference in crack size among the sections in the largest crack-section

In this subsection, the increment of the critical current induced by the difference in crack size among the sections, $\Delta I_{c,ave}$, will be analyzed from the viewpoint of the

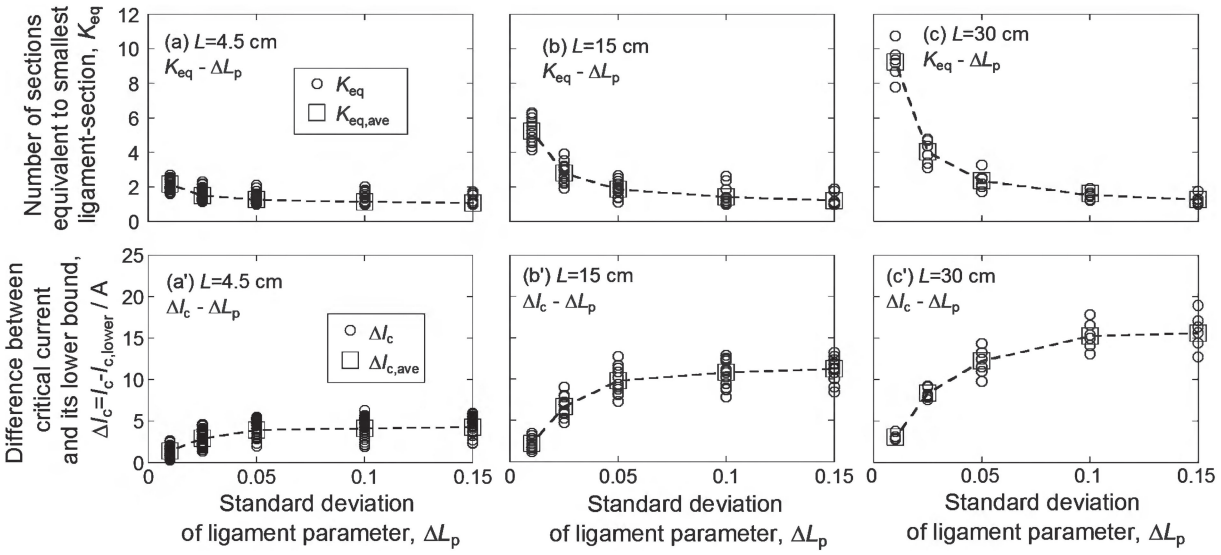

Fig. 8 Plot of (a–c) number of sections equivalent to the smallest ligament (largest crack)-section, K_{eq}, and (a′–c′) difference between the critical current and its lower bound ΔI_c ($= I_c - I_{c,lower}$), against the standard deviation of ligament parameter ΔL_p. (a, a′), (b, b′) and (c, c′) refer to the result for $L = 4.5$, 15 and 30 cm, respectively.

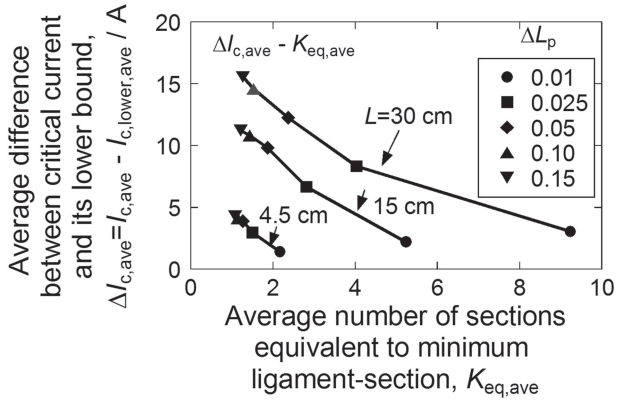

Fig. 9 Average of difference between the critical current and its lower bound, $\Delta I_{c,ave} = I_{c,ave} - I_{c,lower,ave}$, plotted against the average number of sections equivalent to the smallest ligament (largest crack)-section, $K_{eq,ave}$.

contribution of the REBCO layer-transported current $\Delta I_{RE,ave}$ at the ligament part and shunting current $\Delta I_{s,ave}$ at the cracked part in the largest crack-section.

The contributions of $\Delta I_{RE,ave}$ and $\Delta I_{s,ave}$ to the $\Delta I_{c,ave}$ as a function of ΔL_p for $L = 4.5$, 15 and 30 cm were calculated in the following procedure. Substituting the values of $K_{eq,ave}$ obtained by simulation, $I_{c,ave}$ obtained by the calculation procedure stated in the subsection 3.3, specimen length L and $V = V_c = E_c L$ into eq. (8), we obtained the voltage, $V_{RE,ave}$ in the largest crack-section at the critical voltage V_c of the specimen. Then, substituting the $V_{RE} = V_{RE,ave}$ and $L_{p,smallest} = L_{p,smallest,ave}$ calculated by the procedure stated in subsection 3.1 into eq. (9), the $I_{RE,ave}$ given by $I_{c0} L_{p,smallest,ave}\{(V_{RE,ave}/E_c L_0)^{1/n_0}\}$ and the $I_{s,ave}$ given by $V_{RE,ave}/R_t$ were calculated. In the same way, substituting $K_{eq} = K_{eq,ave} = N$, $I_c = I_{c,lower,ave}$, $L_{p,smallest} = L_{p,smallest,ave}$ and corresponding L-value into eqs. (8) and (9), we calculated the $I_{RE,ave}$ and $I_{s,ave}$ for the lower bound $I_{c,lower}$ of critical current. Noting the $I_{RE,ave}$ and $I_{s,ave}$ for the lower bound as $I_{RE,lower,ave}$ and $I_{s,lower,ave}$, respectively, and setting $\Delta I_{RE,ave} = I_{RE,ave} - I_{RE,lower,ave}$ and $\Delta I_{s,ave} = I_{s,ave} - I_{s,lower,ave}$, we had

$$\Delta I_{c,ave} = I_{c,ave} - I_{c,lower,ave} = I_{RE,ave} - I_{RE,lower,ave} + I_{s,ave} - I_{s,lower,ave} = \Delta I_{RE,ave} + \Delta I_{s,ave} \quad (14)$$

From eq. (14), the effects of the difference in crack size among the sections on the increase in average REBCO-transported current in the ligament part, $\Delta I_{RE,ave}$, and the increase in average shunting current in the cracked part $\Delta I_{s,ave}$ in the largest crack-section were evaluated.

Figure 11 shows the increment of critical current from the lower bound, $\Delta I_{c,ave}$ ($= I_{c,ave} - I_{c,lower,ave}$), the increment of the shunting current at the cracked part, $\Delta I_{s,ave}$, and the increment of the REBCO-layer transported current at the ligament part, $\Delta I_{RE,ave}$, in the largest crack-section with increasing ΔL_p for $L = 4.5$, 15 and 30 cm. The following features are read. (i) The phenomenon "the increment of the critical current $\Delta I_{c,ave}$ due to the difference in crack size among the sections becomes large as $K_{eq,ave}$ decreases (Fig. 9)" is attributed to the increase in the shunting current at the cracked part and the current transported by the REBCO layer at the ligament part in the largest crack-section. This is because, with decrease in $K_{eq,ave}$ value, the number of the sections that contribute to the voltage of the specimen decreases and hence the largest crack-section generates a higher voltage at the critical voltage V_c of the specimen at which the critical current is estimated. (ii) This phenomenon becomes more prominent with increasing ΔL_p due to the increase in interspacing among the V–I curves of the sections, which reduces $K_{eq,ave}$-value. Also this phenomenon becomes more prominent for longer specimens due to the increase in V_c ($= E_c L$) which raises $I_{s,ave}$ and $I_{RE,ave}$.

4. Conclusions

(1) The size of the largest crack and also the difference in crack size among the sections affect the critical current value. Model analysis revealed that (i) with increase in standard deviation of crack size, the increase in size of the largest crack acts to reduce critical current and the

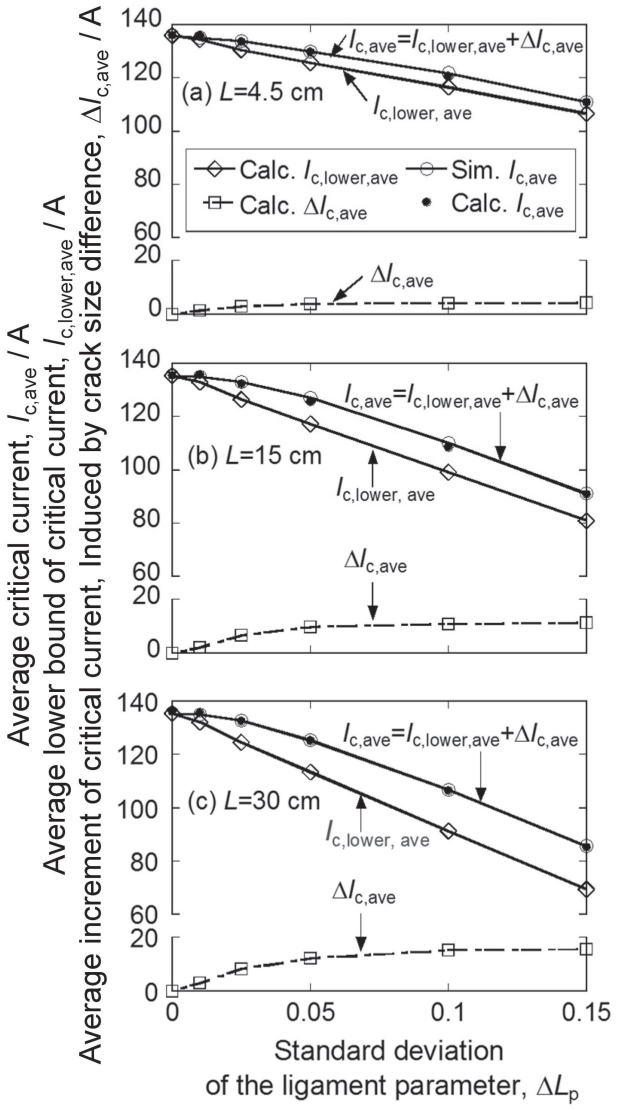

Fig. 10 Effects of the standard deviation of the ligament parameter ΔL_p on average critical current $I_{c,ave}$ obtained by simulation (○) and calculation (●), average lower bound of critical current $I_{c,lower,ave}$ obtained by calculation (◇), and average increment of critical current from the lower bound, $\Delta I_{c,ave}$ ($= I_{c,ave} - I_{c,lower,ave}$), obtained by calculation (□), for specimen length L = (a) 4.5 cm, (b) 15 cm and (c) 30 cm.

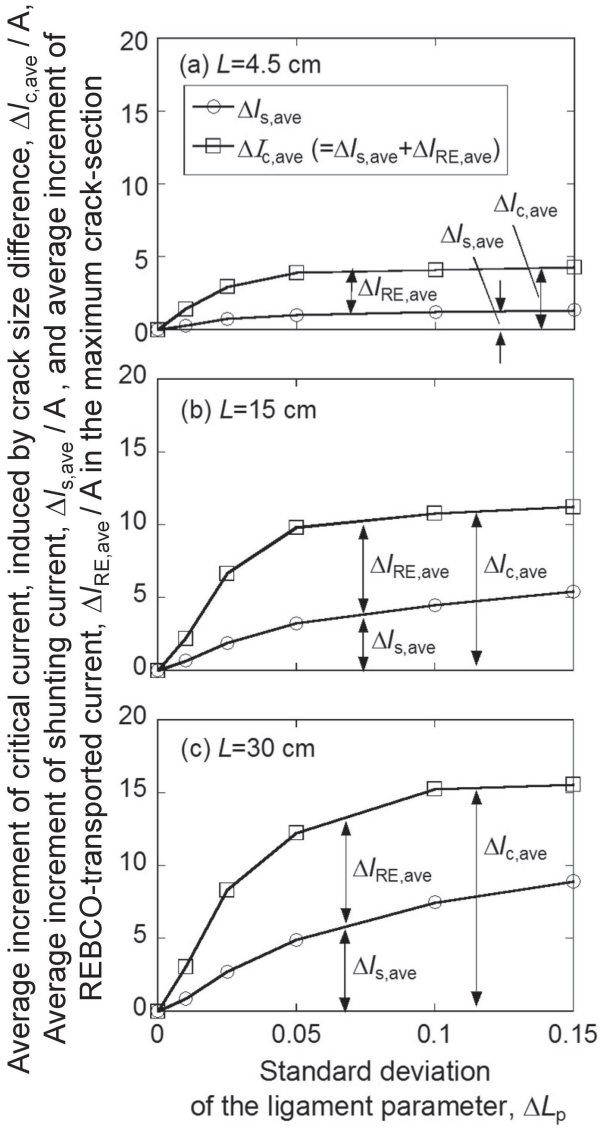

Fig. 11 Average increment of the critical current of specimen $\Delta I_{c,ave}$, and the shunting current $\Delta I_{s,ave}$ and REBCO-layer transported current $\Delta I_{RE,ave}$ in the largest crack-section at $V = V_c = E_c L$, with increasing standard deviation of crack size ΔL_p and specimen length L.

increase in difference in crack size acts to raise the critical current, and (ii) these conflicting two effects are summed up, from which the critical current value is determined.

(2) The largest crack size of the specimen, monitored by the smallest ligament parameter, was obtained based on the Gumbel's extreme value distribution. The difference in crack size among sections was monitored by the number of sections equivalent to the largest crack-section at the critical voltage at which the critical current of the specimen is determined. With these values, the effects of the size of the largest crack and the difference in crack size on critical current value of specimen could be estimated separately.

(3) The analysis of the simulation results with the present approach showed that, when the distribution-width of the size of the cracks contained in the specimen is small and the specimen is short, the size of the largest crack plays a dominant role in determination of the critical current of the specimen, and when the distribution-width of the crack size is large and the specimen is long, both of the largest crack size and the difference in crack size among sections contribute to the determination of critical current value.

REFERENCES

1) D.C. van der Laan, J.W. Ekin, F.F. Douglas, C.C. Clickner, T.C. Stauffer and L.F. Goodrich: Supercond. Sci. Technol. **23** (2010) 072001.
2) S. Ochiai, T. Arai, A. Toda, H. Okuda, M. Sugano, K. Osamura and W. Prusseit: J. Appl. Phys. **108** (2010) 063905.
3) S. Ochiai, H. Okuda, T. Arai, S. Nagano, M. Sugano and W. Prusseit: Cryogenics **51** (2011) 584–590.
4) H.-S. Shin, J. Marlon, H. Dedicatoria, H.-S. Kim, N.-J. Lee, H.-S. Ha and S.-S. Oh: IEEE Trans. Appl. Supercond. **21** (2011) 2997–3000.
5) S. Ochiai, H. Okuda, T. Arai, M. Sugano, K. Osamura and W. Prusseit: J. Japan Inst. Copper **51** (2012) 217–222.
6) H. Oguro, T. Suwa, T. Suzuki, S. Awaji, K. Watanabe, M. Sugano, S.

Machiya, M. Sato, T. Koganezawa, T. Machi, M. Yoshizumi and T. Izumi: IEEE Trans. Appl. Supercond. **23** (2013) 8400304.
7) S. Ochiai, H. Okuda and N. Fujii: Mater. Trans. **58** (2017) 679–687.
8) S. Ochiai, H. Okuda and N. Fujii: Mater. Trans. **58** (2017) 1469–1478.
9) S. Ochiai, H. Okuda and N. Fujii: Mater. Trans. **59** (2018) 1380–1388.
10) S. Ochiai, H. Okuda and N. Fujii: Mater. Trans. **59** (2018) 1628–1636.
11) S. Ochiai, H. Okuda and N. Fujii: Mater. Trans. **60** (2019) 574–582.
12) S. Ochiai and H. Okuda: Mater. Trans. **61** (2020) 213–220.
13) Y. Fang, S. Danyluk and M.T. Lanagan: Cryogenics **36** (1996) 957–962.
14) S. Ochiai, D. Doko, H. Okuda, S.S. Oh and D.W. Ha: Supercond. Sci. Technol. **19** (2006) 1097–1103.
15) S. Ochiai, M. Fujimoto, H. Okuda, S.S. Oh and D.W. Ha: J. Appl. Phys. **105** (2009) 063912.
16) S. Ochiai, M. Fujimoto, J.K. Shin, H. Okuda, S.S. Oh and D.W. Ha: J. Appl. Phys. **106** (2009) 103916.
17) P. Gao and X. Wang: Physica C **517** (2015) 31–36.
18) P. Gao, C. Xin, M. Guan, X. Wang and Y. Zhou: IEEE Trans. Appl. Supercond. **26** (2016) 8401605.
19) Y. Miyoshi, E.P.A. Van Lanen, M.M. Dhallé and N. Nijhuits: Supercond. Sci. Technol. **22** (2009) 085009.
20) G. Nishijima, N. Banno and H. Kitaguchi: IEEE Trans. Appl. Supercond. **25** (2015) 1–4.
21) H. Kitaguchi, A. Matsumoto, H. Hatakeyama and H. Kumakura: Physica C **401** (2004) 246–250.
22) J.J. Gannon, Jr., A.P. Malozemoff, R.C. Diehl, P. Antaya and A. Mori: IEEE Trans. Appl. Supercond. **23** (2013) 8002005.
23) T. Nakamura, Y. Takamura, N. Amemiya, K. Nakao and T. Izumi: Cryogenics **63** (2014) 17–24.
24) E.J. Gumbel: *Statistics of Extremes*, (Columbia Univ. Press, New York, 1958) pp. 156–254.